JOURNAL OF ENVIRONMENTAL SCIENCES 77 (2019) 167–173

Available online at www.sciencedirect.com

ScienceDirect

www.elsevier.com/locate/jes

JES JOURNAL OF ENVIRONMENTAL SCIENCES

www.jesc.ac.cn

Mechanism of oxidation and catalysis of organic matter abiotic humification in the presence of MnO_2

Yingchao Zhang[1], *Dongbei Yue*[1,*], *Xu Wang*[1], *Wenfang Song*[2]

1. *Key Laboratory for Solid Waste Management and Environment Safety (MOE), School of Environment, Tsinghua University, Beijing 100084, China*
2. *Beijing Production and Marketing Service Station for Superiors Agricultural Products, Beijing 100029, China*

ARTICLE INFO

Article history:
Received 28 March 2018
Revised 22 June 2018
Accepted 9 July 2018
Available online 17 July 2018

Keywords:
Abiotic humification
MnO_2
Fulvic-like acids
Humic-like acids
CO_2 release

ABSTRACT

Humification plays a critical role in the environmental fate of organic wastes, and MnO_2 holds great promise for enhancing this reaction. However, the effects of MnO_2 on the enhancement of the humification reaction remain ambiguous. To better reveal the mechanism by which MnO_2 enhances the reaction and investigate the fate of the humification products, abiotic humification experiments were performed using increasing concentrations of dissolved organic matter (DOM) to a fixed amount of MnO_2. DOM was represented by model humic precursors consisting of catechol, glucose and glycine. The results indicate that the reduction of MnO_2 played a dominant role in the formation of fulvic-like acids (FLAs), and the subsequent reduction products, MnOOH and Mn(II), acted as catalysts in the formation of humic-like acids (HLAs). Moreover, CO_2 release occurred during the formation of FLAs, and a strong linear correlation between CO_2 release and the formation of FLAs was observed ($p < 0.01$), where 0.73–1.87 mg of CO_2 was released per mg dissolved organic carbon (DOC) FLAs. Furthermore, the concentration of MnO_2 had a pronounced influence on the product behavior, where a lower MnO_2 concentration decreased the quantity of FLAs produced.

Introduction

Naturally occurring humic substances (HSs) are heterogeneous dark-colored organic macromolecules, resulting from the decay of biomass residues. HSs are composed mainly of fulvic-like acids (FLAs) and humic-like acids (HLAs); FLAs are water-soluble humic materials, whereas HLAs are considered to be soluble in neutral to alkaline media and insoluble in acidic media (Mylonas and Mccants, 1980; Klučáková and Pekař, 2005). Furthermore, the intermediate products of the humification process, which are mainly referred to as FLAs, and exist as HLA polymers, mostly convert to stable HLAs and partially exist in a dynamic equilibrium (Qi et al., 2012; Zhang et al., 2015). Owing to their abundance of active groups such as phenols and carboxylic acids, HSs have functions in agriculture and pollution remediation (Canellas et al., 2015; de Melo et al., 2016; Ren et al., 2017; Jednak et al., 2017). In addition, the humification reaction influences the fate of organic matter and contributes to carbon sequestration (Tan et al., 2017). Therefore, the mechanisms and processes of HSs formation are of great interest (Wei et al., 2014; Vindedahl et al., 2016; Ateia et al., 2017; Potysz et al., 2017; Petrov et al., 2017; Schellekens et al., 2017). During the formation of HSs, polyphenols, amino acids and hydrolyzed sugars can be used as HS precursors to form dark-colored HSs, where the N-containing groups play an important role in the darkening process (Jokic et al., 2004; Nishimoto et al., 2013; Tan, 2014; Pospíšilová et al., 2015; Zhang et al., 2015; Yan and Kim, 2017).

* *Corresponding author. E-mail:* yuedb@tsinghua.edu.cn (Dongbei Yue).

https://doi.org/10.1016/j.jes.2018.07.002
1001-0742/

In addition, the polycondensation reactions of HS precursors are well known to be enhanced by inorganic minerals, especially the active constituents. Metal oxides can be used as Lewis acids to the accept electrons and protons originating from the polycondensation reactions of organic matter (Qi et al., 2012; Li et al., 2012). MnO_2 has been proven to have a paramount role among metal oxides in enhancing the polycondensation reactions of HS precursors by acting as a catalyst (Haruo, 2012). MnO_2 is ubiquitous in nature and is a powerful oxidizing agent by virtue of its high oxidation potential and high specific surface area, thereby promoting the efficient oxidation of HS precursors (Li et al., 2012). Furthermore, the retention of organic matter in nature is mainly controlled by the content of metal oxides. (William and Timothy, 1984). Moreover, the quantity of metal oxides has a tremendous impact on the fate and behavior of carbon conversion (Zech et al., 1997). Electron shuttling between organics and metal oxides has been proposed to occur during humification (Narsito et al., 2010; Nishimoto et al., 2013). As an enhancer, MnO_2 improves the release of protons and electrons from organic matter (Li et al., 2012; de Melo et al., 2015) while also catalyzing the decarboxylation of HS precursors to produce CO_2 and forming HSs during humification (Li et al., 2012). Although numerous studies have proposed mechanisms by which MnO_2 enhances humification, details of the role of MnO_2 in enhancing the formation of HSs remain obscure. Therefore, it is imperative to investigate the effects of MnO_2 on the formation and transformation of FLAs and HLAs and identify the key stage of CO_2 release during humification. Furthermore, the control and conversion of unstable FLAs to stable HLAs are beneficial for improving the quality of recycled biomass waste materials.

This study aimed to investigate the enhancing effects of MnO_2 on the formation of FLAs and HLAs, by using increasing dissolved organic matter (DOM) concentrations with a fixed amount of MnO_2. The DOM was represented by humic precursors, including catechol, glucose and glycine. The formation of humic-like dark-colored polymers during incubation was evaluated by the degree of darkening of the liquid phase (E_{600}). Moreover, the production of FLAs and HLAs associated with CO_2 release was evaluated and quantified by measuring the variations in the dissolved organic carbon (DOC) levels. Furthermore, the relative quantities of FLAs and HLAs were calculated from the ratio between the DOC concentration of each sample and the initial total DOC concentration. Finally, the changes in the structure and concentration of MnO_2 before and after the humification process were investigated with X-ray diffraction (XRD) and inductively coupled plasma-atomic emission spectrometry (ICP-AES).

1. Materials and methods

1.1. Materials and abiotic humification operation

The reagents used in this research have been documented in a previous paper (Zhang et al., 2015). Sterile incubation experiments were performed by adding thimerosal (0.02% W/V) as an antiseptic into 200 mL of autoclaved phosphate buffer, and a pH meter (FE20, Shimadzu, Japan) was used to adjust the pH of the buffer system to 8. Catechol, glucose and glycine were introduced into the phosphate buffer as humic precursors. Glucose and glycine were both added at a concentration of 0.06 mol/L and incubated with increasing catechol concentrations (0, 0.005, 0.01, 0.02, 0.04, 0.06, 0.08, 0.12 mol/L), and 2 g of MnO_2 was also added to each system. The eight reactions, denoted as MR1, MR2, MR3, MR4, MR5, MR6, MR7, and MR8, were performed on a laboratory scale with mass ratios of initial total DOC to Mn: 3.5:1, 4.8:1, 6.1:1, 8.7:1, 13.9:1, 19.1:1, 24.4:1 and 34.8:1. All reactions were conducted in duplicate. Additionally, control 1 consisted of buffer solution only, and control 2 consisted of buffer solution and MnO_2. The samples were incubated in a dark incubator while shaking (150 r/min) at 35°C for 360 hr.

1.2. Characterization of the humification process

Samples with a volume of 1 mL were withdrawn at 0, 3, 6, 18, 28, 48, 76, 124, 172, 240, and 360 hr and centrifuged (10,000 r/min, 10 min) to determine the degree of darkening of the liquid phase (E_{600}), the variations in the DOC level associated with carbon release, and the total Mn concentration in the liquid phase. Samples with a volume of 5 mL were extracted at 0, 18, 48, 76, 124, 172, 240, and 360 hr to quantify the changes in the concentrations of FLAs and HLAs. The withdrawn samples were centrifuged (10,000 r/min, 10 min) using a centrifuge (Kubota 3740, Kubota Corporation, Japan), and filtered (0.45 μm).

1.3. Darkening kinetics

The degree of darkening of the reaction solution (E_{600}) was utilized as an indicator for evaluating the formation of dark-colored polymers of HSs. A 100 μL aliquot of the supernatant was diluted to 10 mL with ultrapure water, and the absorbance at 600 nm was obtained using a UV-1800 ultraviolet–visible spectroscopy (UV–Vis) (UV-1800, Shimadzu, Japan). Another 50 μL aliquot of the supernatant was diluted to 20 mL to determine the concentration of DOC at various sampling times with a total organic carbon (TOC) analyzer (TOC-L CSN, Shimadzu, Japan) The E_{600} was calculated as follows (Qi et al., 2012; Nishimoto et al., 2013):

$$E_{600} = \frac{A_{600}}{\mathrm{DOC(g/L)} \times L\mathrm{(cm)}} \times 1000$$

where A_{600} and L (1 cm) are the absorbance at 600 nm and the length of the light path, respectively.

1.4. Concentrations of FLAs and HLAs

A 5 mL aliquot of the supernatant was acidified to pH 1 with HCl (6 mol/L) and stirred for 24 hr to obtain the precipitate (corresponding to HLAs). The supernatant containing FLAs was passed through a mini-column filled with 1 mL of DAX-8 resin to adsorb the FLAs. After adsorption, the column was washed with approximately 30 mL of ultrapure water, and the FLAs were desorbed with NaOH (0.1 mol/L). The precipitate containing the HLAs was washed with ultrapure water and redissolved with NaOH (0.1 mol/L). Next, the pH of the solutions containing the FLAs and HLAs was adjusted to 7 with HCl (0.1 mol/L) prior to the DOC analysis. After incubation, the final reaction mixture was

centrifuged, and the pH of the supernatant was adjusted to 1.0 to produce a precipitate as described above. To further purify the precipitate, the isolated precipitate was redissolved with NaOH (0.1 mol/L), and the slurry was purified with a mixture of HCl (6% V/V) and HF (6% V/V). The mixture was stirred for 24 hr and then centrifuged (10,000 r/min, 10 min). The precipitate was collected, dialyzed (500 Da), freeze-dried and stored prior to analysis (Zhang et al., 2015).

1.5. Characterization of the humification residues

After the humification reaction, the solid residues from the reactions systems containing the manganese compound were centrifuged (10,000 r/min, 10 min) and separated from the liquid phase. The solid residues were rinsed thoroughly with ultrapure water until the effluent was colorless and then freeze-dried and stored. The phase transformations of MnO_2 in the various systems were analyzed by XRD with a Rigaku diffractometer (RINT 1200-S, Rigaku, Japan) operating at 40 kV and 40 mA with Cu-Kα radiation over an acquisition interval of 5–80°. All powder XRD patterns were analyzed using X' Pert High Score Plus software.

The concentration variations of the total Mn ion dissolution in the supernatant were quantified by ICP-AES (ICPE-9000, Shimadzu, Japan). A 50-μL aliquot of the supernatant was diluted to 10 mL, and an acid mixture of concentrated HNO_3 and H_2O_2 (1/3 V/V) was added in a closed Teflon vessel. Microwave heating was used in the analysis (MARS240150, CEM Corporation, USA). The temperature protocol was as follows: 0–170°C at a rate of 8°C/min, hold at 170°C for 20 min. After digestion, a 4% aqueous solution of H_3BO_3 (10 mL) was added to protect the quartz plasma torch of the ICP-AES instrument. Finally, the samples were analyzed by ICP-AES.

2. Results and discussion

2.1. Humification process

2.1.1. Darkening process of humification

As shown in Fig. 1, E_{600} initially exhibited an increasing trend in systems MR2–MR8, and later showed a slower growth period until approximately 74 hr as the reaction progressed. Note that the highest E_{600} value was observed in MR4 at 74 hr, while when the DOM concentration increased further, a dramatic decline in E_{600} was observed in MR5 after 74 hr. The changes presented above demonstrate that increasing the DOM concentration contributed to the formation of darkening substances within a certain range. However, as more DOM was added, the humification path may have changed. Meanwhile, the E_{600} values of MR6, MR7 and MR8 displayed a remarkably lower rate of change than the other systems and a decrease during the early stage of the reaction. This decrease was attributed to the introduction of an excessive amount of DOM, which led to a disproportionate amount of reactant and further affected the enhancer, which can improve humification and in turn decelerate the darkening reaction. In addition, in systems MR7 and MR8, the E_{600} values remained relatively constant, indicating that the superfluous DOM was not helpful for promoting the darkening reaction.

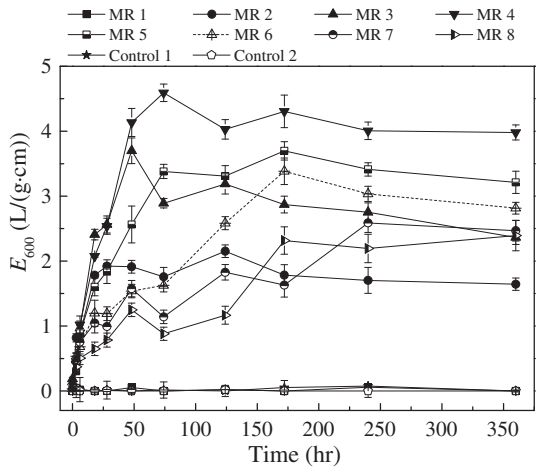

Fig. 1 – Darkening process of humic substance (HS) precursor polymerization. E_{600}: the degree of darkening of the liquid phase; MR1, MR2, MR3, MR4, MR5, MR6, MR7 and MR8 represent dissolved organic carbon (DOC)-to-Mn mass ratios of 3.5:1, 4.8:1, 6.1:1, 8.7:1, 13.9:1, 19.1:1, 24.4:1 and 34.8:1, respectively. Control 1 consisted of buffer solution only, and Control 2 consisted of buffer solution and MnO_2.

2.1.2. Concentrations of FLAs and HLAs

In system MR1 and the controls (not shown), no humification occurred, as shown by the variations (or lack thereof) in E_{600}. As shown in Fig. 2, as the DOM concentration increased, the FLA concentration reached the second highest level at 18 hr in MR4, and the overall highest concentration of FLAs was observed in MR5. However, as the DOM concentration was increased further, interestingly, the FLA concentrations exhibited a remarkable downward trend, indicating that the introduction of an excessive amount of DOM was not conducive to increasing the amount of FLAs produced. Additionally, the FLA content remained nearly constant at the end of the humification reaction, suggesting that a dynamic balance of FLAs may have been reached in which HLAs were generated and transformed, and a portion of the unstable FLAs were converted to carbon dioxide (Zech et al., 1997; Reemtsma et al., 2006).

Meanwhile, the HLA yield and the corresponding reaction rate increased as more DOM was introduced, which can be seen from systems MR2 to MR4. However, the reaction rate during the initial reaction stage dropped significantly in MR5. In addition, the HLA content and reaction rate exhibited sluggish growth in MR7 and MR8, further illustrating that the amount of active ingredients related to humification was far from sufficient for utilizing more DOM in the reaction. Notably, an increase in the DOM concentration could lead to an unbalanced reaction ratio of the HS precursors. Although the intra-/intermolecular polymerization at a high catechol concentration could increase the yield of HLAs, the content of HLAs showed little increase as humification progressed, which can be seen from systems MR6 to MR8.

Considering the variations described above, a key turning point in the amount of DOM emerged near MR5, after which increasing the level of DOM led to an imbalanced reactant mole ratio. Based on the changes in E_{600}, FLA and HLA concentrations, it was postulated that insufficient MnO_2 was present in the reaction, which possibly resulted in the inhibition of electron

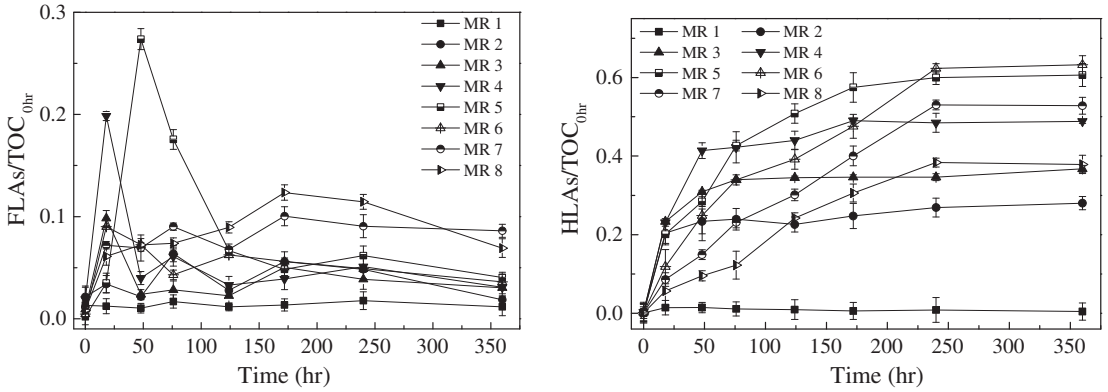

Fig. 2 – Formation of fulvic-like acids (FLAs) and humic-like acids (HLAs). $TOC_{0\ hr}$: the initial concentration of dissolved organic matter (DOM) measuring by dissolved organic carbon (DOC) levels at 0 hr.

transfer and mediated the fate and behavior of FLAs, which in turn affected the production of HLAs.

2.1.3. Total Mn ion dissolution and CO_2 release

The content of metal oxides/hydroxides is important for controlling the humification and mineralization of organic matter (William and Timothy, 1984; Zech et al., 1997). Therefore, the content of water-extractable Mn and the total Mn concentration were determined at the end of the reaction. The total Mn dissolution and CO_2 release were investigated by statistical analysis. The results showed a strong linear correlation ($p < 0.05$), where increasing Mn dissolution is conducive to introducing more organic carbon into the humification reaction, thereby accelerating the formation of darkening substances, which is consistent with the changes in E_{600}. Additionally, Mn ions were present in the liquid phase, which further supported the hypothesis that MnO_2 was involved in the humification reaction, and that this function of MnO_2 affected the formation of FLAs and/or HLAs concomitant with CO_2 generation. Moreover, the observed reduction in the DOM content may have occurred through CO_2 release (Zech et al., 1997). However, the specific causes of CO_2 release are still under investigation. The regression line is illustrated in Fig. 3.

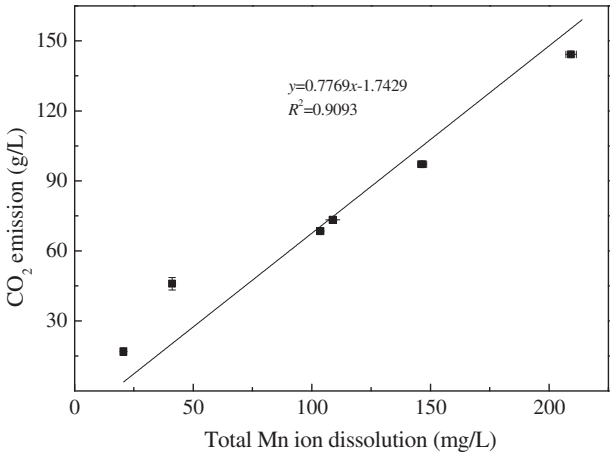

Fig. 3 – Linear regression between total Mn dissolution and total CO_2 release.

2.2. Residue analysis

As shown in Fig. 4, the variations in the XRD patterns clearly revealed that humification was susceptible to the effects of the phosphate buffer, including the disappearance of MnO_2 and the appearance of new phases, where the following phases of MnO_2 were identified: MnO_2, $Mn_3(PO_4)_2{\cdot}3H_2O$, $NH_4MnPO_4{\cdot}H_2O$ and MnOOH (Danvirutai et al., 2010; Lin and Wang, 2011; Jin et al., 2014). The valence states of Mn in system MR1 and the control groups were in accordance with that of the initial MnO_2. $Mn_3(PO_4)_2{\cdot}3H_2O$ appeared in MR1, while the peak intensity of MnO_2 was weakened, indicating that MnO_2 was involved in the reaction. Note that the valence state of Mn changed as the DOM content increased, and the valence states of Mn were markedly different in MR4, revealing that electrons were transferred. $NH_4MnPO_4H_2O$, MnOOH and $Mn_3(PO_4)_2{\cdot}3H_2O$ were identified as the main components, and less MnO_2 was observed. However, as the DOM content increased, the MnO_2 content decreased and disappeared in MR5, which was accompanied by an obvious increase in the intensity of the crystalline peaks corresponding to MnOOH and $Mn_3(PO_4)_2{\cdot}3H_2O$. However, as the amount of DOM further increased in MR6, MR7 and MR8, $Mn_3(PO_4)_2{\cdot}3H_2O$ dominated the final solid residues.

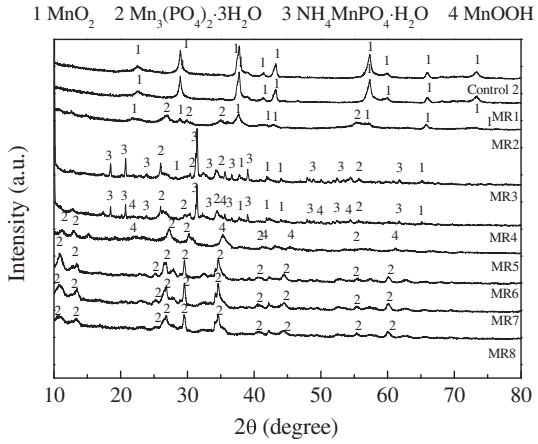

Fig. 4 – X-ray diffraction (XRD) patterns of the end solid residues.

The XRD results demonstrated that Mn ions existed in three oxidation states during humification: Mn(IV), Mn(III) and Mn(II). This result indicated that the amount of MnO_2 was not sufficient to promote the transfer of electrons and protons as the DOM content increased. Moreover, the appearance of various valence states of Mn was attributed to the reduction of Mn(IV) to Mn(III) and Mn(II) during the oxidative polymerization and cleavage of the HS precursors (Hardie et al., 2009; Narsito et al., 2010; Nishimoto et al., 2013), which in turn affected the formation of HSs. Furthermore, based on the combination of the above analyses, three critical DOM levels clearly emerged: those in systems MR4, MR5 and MR6. Increasing the DOM content to that in MR4 was beneficial for forming darkening substances and concomitantly accelerating the reaction. However, when the DOM content was further increased to that in MR5, a downward trend appeared in the reaction rate. Although E_{600} continued to increase, the content of FLAs increased to the maximum value of 0.274 (48 hr); meanwhile, the rate of HLA formation began to decrease. However, as the DOM content was increased to that in MR6 and beyond, E_{600} exhibited a rapidly deceasing trend, the levels of FLAs and HLAs formed were distinctly lower, and the reaction rate was slower. The dynamic variations in E_{600} and the HSs further supported the hypothesis that MnO_2 plays a crucial role in abiotic humification. Therefore, the entire humification performance was confirmed to be predominantly driven by the amount of MnO_2.

2.3. Kinetic analysis

Based on the aforementioned study, FLAs were formed as intermediate products during the formation of HLAs, and the entire humification reaction can be divided into two parts, transformation of the HS precursors into FLAs and conversion of the FLAs into HLAs. The formation of FLAs, HLAs, and the related CO_2 can be described by and evaluated with the proposed equations below:

$$\mathrm{DOM} \xrightarrow{k_1} \mathrm{FLAs} + m\mathrm{CO_2} \quad (1)$$

$$\mathrm{FLAs} \xrightarrow{k_2} \mathrm{HLAs} + n\mathrm{CO_2} \quad (2)$$

$$[\mathrm{CO_2}] = ([\mathrm{FLAs}] + [\mathrm{HLAs}]) \times m\,[\mathrm{CO_2}] + [\mathrm{HLAs}] \times n\,[\mathrm{CO_2}] \quad (3)$$

where, DOM represents the initial HS precursors, and FLAs and HLAs are the intermediate and final products of humification, respectively. k_1 (L/(mg·hr) and k_2 (mg/(L·hr)) represent the kinetic constants of the two steps in the formation of FLAs and HLAs, respectively. $[CO_2]$ is the amount of CO_2 molecules released (mg/mg DOC [FLAs] and/or [HLAs]), and [FLAs] and [HLAs] are the concentrations of FLAs and HLAs (mg DOC/L), respectively. Moreover, m and n are the numbers of CO_2 molecules generated and evolved during the formation of each molecule of FLAs and HLAs, respectively. However, the fitting results showed that n was invalid ($m > 0$, $n < 0$), indicating that the CO_2 was released during FLA evolution. Therefore, the number of CO_2 molecules released was calculated with the following formula:

$$[\mathrm{CO_2}] = ([\mathrm{FLAs}] + [\mathrm{HLAs}]) \times m\,[\mathrm{CO_2}] \quad (4)$$

The related m value was determined and gave a CO_2 release amount of 0.73–1.87 mg/mg DOC of FLAs formed. In addition, the related kinetic equations were determined using a kinetic model, and the reaction rates were evaluated in terms of k_1 and k_2. The calculations of k_1 and k_2 echoed the calculations of previous studies (Zhang et al., 2015), and the corresponding reaction constants are summarized in Table 1. The obtained results show that the formation of FLAs and HLAs respectively followed pseudo-second-order and zero-order kinetics models well. Accordingly, based on the results shown in Table 1, combined with the previous analysis of the increases in the DOM content up to the levels in MR6, the amount of MnO_2 was sufficient for oxidizing HS precursors and forming FLAs, resulting in a lower reaction rate, which can be seen from the variations in k_1. Note that in the presence of a considerable amount of MnO_2, k_1 remained stable, which can be seen from the changes in the equilibrium constant from MR2 to MR5. However, as the concentration of DOM increased further, k_1 was reduced by roughly one order of magnitude below that of system MR5, demonstrating that the presence of an inadequate amount of MnO_2 impeded the formation of FLAs. Thus, MnO_2 was strongly involved in the formation of FLAs, and the amount of MnO_2 had a profound influence on the behavior and fate of the FLAs. In contrast, k_2 remained nearly constant in the various systems, indicating that the reduction products of MnO_2, Mn(III) and Mn(II), were formed during the formation of FLAs but had little impact on the formation of HLAs, and possibly functioned as catalysts to facilitate the production of HLAs.

Based on the combined changes in the FLA and HLA contents observed throughout the humification reaction, CO_2 release was related to the formation of FLAs, demonstrating that oxidative polymerization of the HSs precursors occurred to form FLAs through oxidization by MnO_2. Consequently, DOM reduction occurred in two steps. The oxidative polycondensation of the HS precursors occurred during the formation of the FLAs and was associated with CO_2 release, and a portion of the less-stable FLAs

Table 1 – Reaction rate constants of abiotic humification.

	MR2	MR3	MR4	MR5	MR6	MR7	MR8
k_1 (L/(mg·hr))	1.12×10^{-6}	2.00×10^{-6}	2.00×10^{-6}	1.02×10^{-6}	6.00×10^{-7}	3.00×10^{-7}	1.00×10^{-7}
R^2	0.7170	0.8088	0.8985	0.7220	0.9097	0.8978	0.9882
k_2 (mg/(L·hr))	24.5	34	32.1	37.5	88.8	52	59.4
m	1.39 **	1.87 **	1.39 **	0.84 **	0.73 **	1.14 **	1.28 **

m: the number of CO_2 molecules released per molecule of FLA formed; k_1 and k_2 represent the kinetic constants of the two steps in the formation of FLAs and HLAs, respectively. R^2 was the fitting correlation coefficient for k_1, and k_2 was calculated according to the tandem reaction kinetics equation without further fitting correlation, therefor R^2 for k_2 is meaningless.
** $p < 0.01$.

was oxidized to CO_2 (Reemtsma et al., 2006). Mn(IV) oxides induced the formation of free radicals and consumed the protons and electrons formed from the oxidative polymerization of the HS precursors (Hardie et al., 2007; Chen et al., 2010), thereby reducing Mn(IV) to Mn(III) and Mn(II), which led to the formation of polycarboxylic FLAs. Furthermore, polymerization continued as the FLAs were converted to HLAs in a process catalyzed by the dissolved Mn ions. Therefore, the following possible mechanisms for the abiotic humification of organic matter enhanced by MnO_2 were proposed: The HS precursors were first oxidized to FLAs in a process associated with the release of CO_2, and those FLAs were then converted to HLAs in a reaction catalyzed by the produced Mn ions.

3. Conclusions

This study highlights the oxidation and catalytic mechanisms of MnO_2 and the related reduction products in enhancing abiotic humification. The significant contribution of the MnO_2 levels to the formation of FLAs was investigated, and meanwhile, the release of carbon dioxide associated with the formation of FLAs was elucidated, where 0.73–1.87 mg of CO_2 was produced per mg of DOC FLAs. The reduction products Mn(III) and Mn(II) functioned as catalysts to convert the FLAs to HLAs. Therefore, to transform more unstable FLAs into HLAs while also reducing the amount of CO_2 released, the ratio between the metal oxide and organic matter should be effectively controlled, which will also improve the quality of the biomass waste recycling process and increase carbon sequestration.

Acknowledgments

The authors are grateful for the financial support from the National Key Technology R&D Programs (No. 2014BAC02B02).

REFERENCES

Ateia, M., Ran, J., Fujii, M., Yoshimura, C., 2017. The relationship between molecular composition and fluorescence properties of humic substances. Int. J. Environ. Sci. Technol. 14 (4), 867–880.

Canellas, L.P., Olivares, F.L., Aguiar, N.O., Jones, D.L., Nebbioso, A., Mazzei, P., et al., 2015. Humic and fulvic acids as biostimulants in horticulture. Sci. Hortic. 196, 15–27.

Chen, Y.M., Tsao, T.M., Liu, C.C., Huang, P.M., Wang, M.K., 2010. Polymerization of catechin catalyzed by Mn-, Fe- and Al-oxides. Colloids Surf. B 81, 217–223.

Danvirutai, C., Noisong, P., Youngme, S., 2010. Some thermodynamic functions and kinetics of thermal decomposition of $NH_4MnPO_4{\cdot}H_2O$ in nitrogen atmosphere. J. Therm. Anal. Calorim. 100, 117–124.

de Melo, B.A.G., Motta, F.L., Santana, M.H.A., 2015. The interactions between humic acids and Pluronic F127 produce nanoparticles useful for pharmaceutical applications. J. Nanopart. Res. 17, 1–11.

de Melo, B.A.G., Motta, F.L., Santana, M.H.A., 2016. Humic acids: structural properties and multiple functionalities for novel technological developments. Mater. Sci. Eng. C 62, 967–974.

Hardie, A.G., Dynes, J.J., Kozak, L.M., Huang, P.M., 2007. Influence of polyphenols on the integrated polyphenol-Maillard reaction humification pathway as catalyzed by birnessite. Ann. Environ. Sci. 1, 91–110.

Hardie, A.G., Dynes, J.J., Kozak, L.M., Huang, P.M., 2009. Biomolecule-induced carbonate genesis in abiotic formation of humic substances in nature. Can. J. Soil Sci. 89, 445–453.

Haruo, S., 2012. Relative effectiveness of short-range ordered Mn (IV), Fe(III), Al, and Si oxides in the synthesis of humic acids from phenolic compounds. Soil Sci. Plant Nutr. 38, 459–465.

Jednak, T., Avdalović, J., Miletić, S., Slavković-Beškoski, L., Stanković, D., Milić, J., et al., 2017. Transformation and synthesis of humic substances during bioremediation of petroleum hydrocarbons. Int. Biodeterior. Biodegrad. 122, 47–52.

Jin, K., Park, J., Lee, J., Yang, K.D., Pradhan, G.K., Sim, U., et al., 2014. Hydrated manganese(II) phosphate ($Mn_3(PO_4)_2{\cdot}3H_2O$) as a water oxidation catalyst. J. Am. Chem. Soc. 136, 7435.

Jokic, A., Wang, M.C., Liu, C., Frenkel, A.I., Huang, P.M., 2004. Integration of the polyphenol and Maillard reactions into a unified abiotic pathway for humification in nature. Org. Geochem. 35, 747–762.

Klučáková, M., Pekař, M., 2005. Solubility and dissociation of lignitic humic acids in water suspension. Colloids Surf. A 252, 157–163.

Li, C., Zhang, B., Ertunc, T., Schaeffer, A., Ji, R., 2012. Birnessite-induced binding of phenolic monomers to soil humic substances and nature of the bound residues. Environ. Sci. Technol. 46, 8843–8850.

Lin, W., Wang, D.L., 2011. Preparation and electrochemical characterization of MnOOH nanowire–graphene oxide. Electrochim. Acta 56, 5010–5015.

Mylonas, V.A., Mccants, C.B., 1980. Effects of humic and fulvic acids on growth of tobacco. 2. Tobacco growth and ion uptake. J. Plant Nutr. 2, 377–393.

Narsito, N., Santosa, S.J., Lastuti, S., 2010. Photo-reduction kinetics of MnO_2 in aquatic environments containing humic acids. Indones. J. Chem. 8.

Nishimoto, R., Fukuchi, S., Qi, G., Fukushima, M., Sato, T., 2013. Effects of surface Fe(III) oxides in a steel slag on the formation of humic-like dark-colored polymers by the polycondensation of humic precursors. Colloids Surf. A 418, 117–123.

Petrov, D., Tunega, D., Gerzabek, M.H., Oostenbrink, C., 2017. Molecular dynamics simulations of the standard Leonardite humic acid: microscopic analysis of the structure and dynamics. Environ. Sci. Technol. 51, 5414.

Pospíšilová, L., Komínková, M.T., Zítka, O.E., Kizek, R., Barančíková, G., Litavec, T.Å., et al., 2015. Fate of humic acids isolated from natural humic substances. Acta Agric. Scand. 65, 517–528.

Potysz, A., Grybos, M., Kierczak, J., Guibaud, G., Fondaneche, P., Lens, P.N., et al., 2017. Metal mobilization from metallurgical wastes by soil organic acids. Chemosphere 178, 197–211.

Qi, G., Yue, D., Fukushima, M., Fukuchi, S., Nishimoto, R., Nie, Y., 2012. Enhanced humification by carbonated basic oxygen furnace steel slag — II. Process characterization and the role of inorganic components in the formation of humic-like substances. Bioresour. Technol. 114, 637–643.

Reemtsma, T., These, A., Springer, A., Linscheid, M., 2006. Fulvic acids as transition state of organic matter: indications from high resolution mass spectrometry. Environ. Sci. Technol. 40, 5839–5845.

Ren, D., Huang, B., Yang, B., Pan, X., Dionysiou, D.D., 2017. Mitigating 17α-ethynylestradiol water contamination through binding and photosensitization by dissolved humic substances. J. Hazard. Mater. 327, 197–205.

Schellekens, J., Buurman, P., Kalbitz, K., Zomeren, A.V., Vidal-Torrado, P., Cerli, C., et al., 2017. Molecular features of humic acids and fulvic acids from contrasting environments. Environ. Sci. Technol. 51, 1330–1339.

Tan, K.H., 2014. Humic Matter in Soil and the Environment: Principles and Controversies. CRC Press.

Tan, Y., Yang, W., Liao, S., Peng, Y., Jun, L.I., Fuzhong, W.U., 2017. Effects of soil fauna on winter litter humification along an altitudinal gradient in cold ecosystems in western Sichuan. Acta Ecol. Sin. 37.

Vindedahl, A.M., Stemig, M.S., Arnold, W.A., Penn, R.L., 2016. Character of humic substances as a predictor for goethite nanoparticle reactivity and aggregation. Environ. Sci. Technol. 50.

Wei, X., Shao, M., Du, L., Horton, R., 2014. Humic acid transport in saturated porous media: influence of flow velocity and influent concentration. J. Environ. Sci. (China) (12), 2554–2561.

William, H., Timothy, 1984. Podzolization: soil processes control dissolved organic carbon concentrations in stream water. Soil Sci. 137, 23–32.

Yan, G., Kim, G., 2017. Speciation and sources of brown carbon in precipitation at Seoul, Korea: insights from excitation–emission matrix spectroscopy and carbon isotopic analysis. Environ. Sci. Technol. 51 (20).

Zech, W., Senesi, N., Guggenberger, G., Kaiser, K., Lehmann, J., Miano, T.M., Miltner, A., Schroth, G., 1997. Factors controlling humification and mineralization of soil organic matter in the tropics. Geoderma 79, 117–161.

Zhang, Y., Yue, D., Ma, H., 2015. Darkening mechanism and kinetics of humification process in catechol-Maillard system. Chemosphere 130, 40–45.